**TECHNISCHE
UNIVERSITÄT
DRESDEN**

Sensitivity of dim 8 EFT operators to resonance signals in Vector scattering boson scatterings

Bachelor-Arbeit
zur Erlangung des Hochschulgrades
Bachelor of Science
im Bachelor-Studiengang Physik

vorgelegt von

Georg Schmieder
geboren am 14.10.1996 in Oschersleben

Institut für Kern und Teilchen Physik
Fakultät Physik
Bereich Mathematik und Naturwissenschaften
Technische Universität Dresden
2022

Eingereicht am xx. Monat 20xx

1. Gutachter: Dr. Frank Siegert
2. Gutachter: Prof. Dr. Arno Straessner

Summary

Abstract
English:

Abstract
Deutsch

Contents

1 Introduction

2 Theoretical Foundation
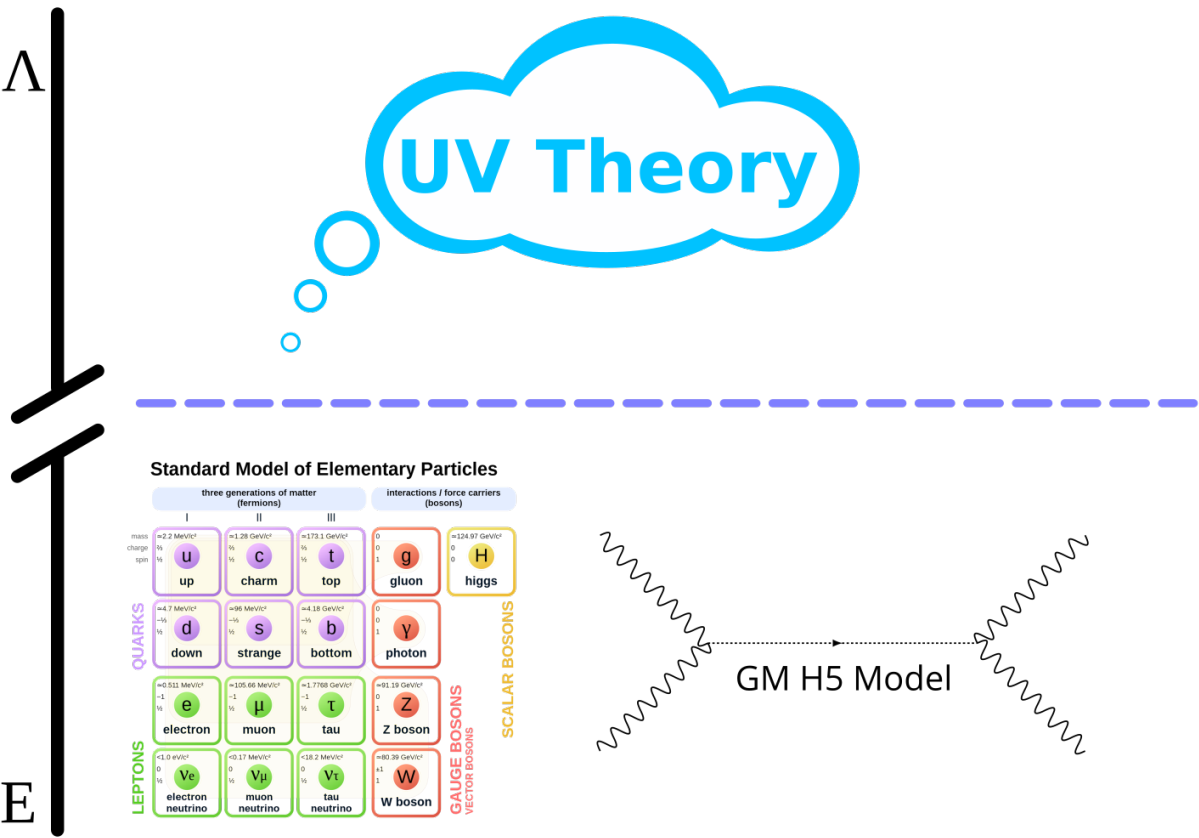
2.1 Effective Field Theory

Figure 2.1: Source and text [**Brivio.2017**]

With the Standard Model Physicist try to describe the elementary Particles and interactions. It is successful in describing most processes in Biology, Chemistry, and Physics. But the Standard Model is still incomplete. It can't describe Phenomenons like Gravity, Neutrino Masses, Matter-Antimatter asymmetry etc. This is where effective field theory comes in. Here we look at the Standard Model as a low energy approximation of an underlying Ultraviolet Theory (figure **??**).

The concept of an Effective Field Theory(EFT) can be Illustrated in different ways using

the Euler-Heisenberg Lagrangian, the Fermi theory or the Standard Model Effective Field Theory(EFT). [**Pich.1998**] shows The Euler-Heisenberg Lagrangian and the Fermi theory while I will be focusing on the SMEFT, as the Name suggests The SMEFT aims to extant the Standard Model. Except the g-Faktor of the Myon the Standard Model has been robust without meaningful deviations from Experimental Measurements. There using a theory that keeps the $SU(3) \times SU(2) \times U(1)$ symmetry with the Higgs field breaking gauge symmetry is desirable. Therefore, we construct the Lagrangian from the gauge invariance for Standard Model fields but allow arbitrarily large mass dimensions. With that any SMEFT Lagrangian can be written as:

$$\mathcal{L}_{SMEFT} = \mathcal{L}_{SM} + \frac{1}{\Lambda}\mathcal{L}_5 + \frac{1}{\Lambda^2}\mathcal{L}_6 + \frac{1}{\Lambda^3}\mathcal{L}_7 + \frac{1}{\Lambda^4}\mathcal{L}_8 + ... \text{ with } \mathcal{L}_i = \sum_i c_i^D \mathcal{O}_i^D \tag{2.1}$$

The operators $\mathcal{O}_i$ are constructed from the Gauge invariance of the SM fields while the Wilson coefficients c_i contain the information on heavy degrees of freedom. Normally the heavy degrees of freedom are integrated out to have a renomilazible Theory but are needed to describe high energy Particles. We get the Wilson coefficients from the operator product expansion in 2.1. Again a good example for the operator product expansion is the Fermi Theory shown in [**Pich.1998**]. For a characteristic heavy scale Λ the operators are ordered by there dimension d_i fixing the dimension of their respective coefficients.
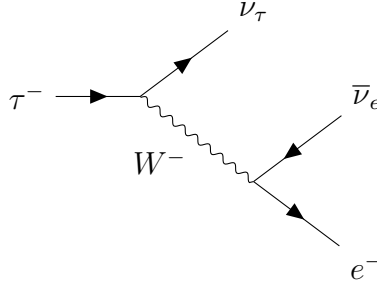
$$[\mathcal{O}_i] = d_i \longrightarrow c_i \sim \frac{1}{\Lambda^{d_i-4}} \tag{2.2}$$

The Leading order $D = 4$ term in 2.1 is the SM Lagrangian while deviations of the SM are described by operators with a dimension $D > 4$.

2.1.1 Fermi Theory on the example Tau Decay

Enrico Fermi proposed 1933 the Fermi Theory in order to describe the β-decay. His theory was able to describe the weak coupling quite well without the former knowledge about the $W^\pm$-Boson which was only later theorized in 1968 by Steven Weinberg, Sheldon Glashow and Abdus Salam. The $W^\pm$-Boson was finally discovered in 1983. 50 years after Fermi's first successful description of an Interaction involving the $W^\pm$-Boson. Today we would call the Fermi theory the low-energy effective field theory of $W^\pm$-Boson. Let us now try to create our own Fermi Theory but instead of describing the β decay we will look at the τ-decay specifically the decay mode $\tau \to \nu_\tau e^- \nu_e$. Even though we are technically cheating since Fermi didn't have our knowledge about the tensor structure of the Weak interaction in Quantum Field Theory or our knowledge about Feynman diagrams. We will start by drawing the Feynamn Diagramm

and writing down the Matrix element.

$$-i\mathcal{M}_{fi} = \left[\frac{g_W}{\sqrt{2}} \overline{u}(k_{\nu_\tau}) \frac{1}{2} \gamma^\mu (1 - \gamma^5) u(k_\tau) \right] \frac{g_{\mu\sigma} - \frac{k_\nu k_\sigma}{m_W^2}}{k^2 - m_W^2} \left[\frac{g_W}{\sqrt{2}} \overline{u}(k_e) \frac{1}{2} \gamma^\sigma (1 - \gamma^5) v(k_{\overline{\nu_e}}) \right] \quad (2.3)$$

In most low ernergy decay processes the momentum of the intermediate W^--Boson is small compared to its mass. Therefore, we can approximate the propagator(2.4) in Orders of the momentum k but we will be writing it in the Matrixelement in Orders of mass since these are more interesting to us. In the Feynman Diagramm this can be expressed by collapsing the properagtor into a single Vertex.
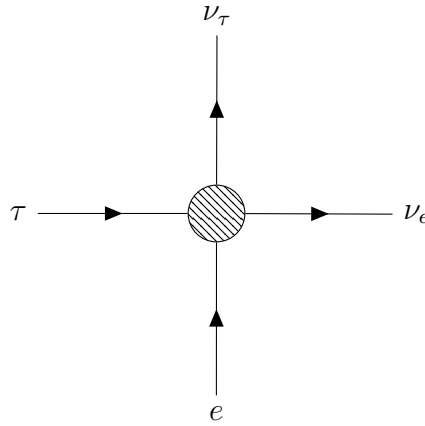
$$\frac{-ig_{\mu\sigma} - \frac{k_\nu k_\sigma}{m_W^2}}{k^2 - m_W^2} \xrightarrow{|q|^2 \ll m_W^2} \frac{ig_{\mu\sigma}}{m_W^2} \left(1 + \frac{k^2}{m_w^2} + \frac{k^4}{m_W^6} + \mathcal{O}(k^6) \right) \quad (2.4)$$

$$\Rightarrow i\mathcal{M}_{fi} = \frac{g_W^2}{8m_W^2} \left[\overline{u}(k_{\nu_\tau}) \gamma^\mu (1 - \gamma^5) u(k_\tau) \right] g_{\mu\sigma} \left[\overline{u}(k_e) \gamma^\sigma (1 - \gamma^5) v(k_{\overline{\nu_e}}) \right] + \mathcal{O}(m_W^4) \quad (2.5)$$

Let us now compare our result with the result Fermi would have gotten if he knew about the parity violation discovered by Wu in 1957.

$$i\mathcal{M}_{fi} = \frac{G_F}{\sqrt{2}} \left[\overline{u}(k_{\nu_\tau}) \gamma^\mu (1 - \gamma^5) u(k_\tau) \right] g_{\mu\sigma} \left[\overline{u}(k_e) \gamma^\sigma (1 - \gamma^5) v(k_{\overline{\nu_e}}) \right] \quad (2.6)$$

With $G_F \approx 4.5437957 \times 10^{14} J^{-2}$ being the Fermi constant which is typically measured in the muon decay. The $1/\sqrt{2}$ is added in order to not change the numerical value of G_F while considering the parity violation. From equation 2.5 and 2.6 we get the following result.

$$\frac{G_F}{\sqrt{2}} = \frac{g_W^2}{8m_W^2} \tag{2.7}$$

Defining the expansion scale $\Lambda = m_W$ and the Wilson coefficient $c = \frac{g_W^2}{8}$ we can see that the Matrix element has dimension 2. With this we can also write down a new effective Lagrangian without the $W^\pm$-Boson but. The EFT described has to contain the tau, electron, their respective neutrienofields as well as the Interaction Lagrangian.

$$\mathcal{L}_{EFT} = \frac{c}{\Lambda^2} \left(\overline{\nu}_\tau \overline{\gamma}_\rho \tau \right) \left(\overline{e} \gamma_\rho \nu_e \right) + \mathcal{O}(\frac{1}{\Lambda^4}) \tag{2.8}$$

Our Fermi Theory is only valid for low energies since Scattering Amplitude from the Standard Model and the EFT would start to diverge once the Energy gets close to the mass of the $W^\pm$-Boson. The m_W defines the validity scale of the EFT in this case the Fermi Theory. For Energies higher than m_W the Fermi Theory is no longer valid. We can increase the validity scale by including therms of higher dimension in Λ. In this example we derived the Matrix element from the SM and then compared the result with the result from Fermi in order to determine $\frac{c}{\Lambda}$. This requires knowledge about the UV theory which is not accessible in low-Energy Measurements. As a result we have to make assumptions about a UV Theory in order to construct the right EFT.

2.2 BSM Theories

In 2012 the last particle predicted by the SM was detected at CERN the Higgs Boson. Yet again proving the success of the SM. But this also means no more free parameters in the SM for new particles. All interactions found obey the local $SU(3) \times SU(2) \times U(1)$ gauge symmetries and later data only strengthens the SM prediction. While no data was found suggesting inconsistencies with the electroweak symmetry breaking $SU(2) \times U(1) \rightarrow U(1)$. This means physicist have to search for new interactions considering different interaction ranges and strengths(Figure 2.2).

(a) Considerably weaker than gravitation with infinite range

(b) Shorter range than the weak interaction of any strength

(c) Range between weak interaction and nuclear force and considerably weaker than the weak interaction
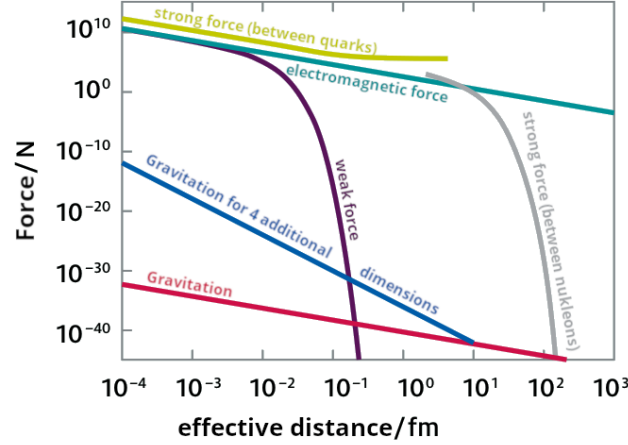
Figure 2.2: Interaction strength for different ranges of the Fundamental interactions. Although the Nuclear force isn't a fundamental it is shown in order to visualize point (c). Translation of the interaction

There are various methods for finding BSM particles and as many theoretical models for new interactions, but these can generally be broken down in three categories.

The Model specific search where one takes a well-defined model often describing a complete UV theory and try's to find the predicted particles in measurements. The most popular example for this is the Supersymmetry which is often associated with the search for Dark Matter and adds a wide range of different particles. In the search for Dark Matter one would look for example look for missing transverse momentum in top quark interactions or look for resonance with the so-called two Higgs doublet models.

Another way of looking for new physics is by using simplified Models. Here one takes a well-defined model in order to describe some aspects or specific phenomenon of the UV Theory. Again a good example comes from dark matter physics the beautifully named neutralino in Minimale Supersymmetry Standard Model(MSSM) with MSSM being a low energy model of the Supersymmetry. Here the for neutralinos are electrically neutral fermions with a mass over 300 GeV and conserves the hypothetical R-parity in MSSM.
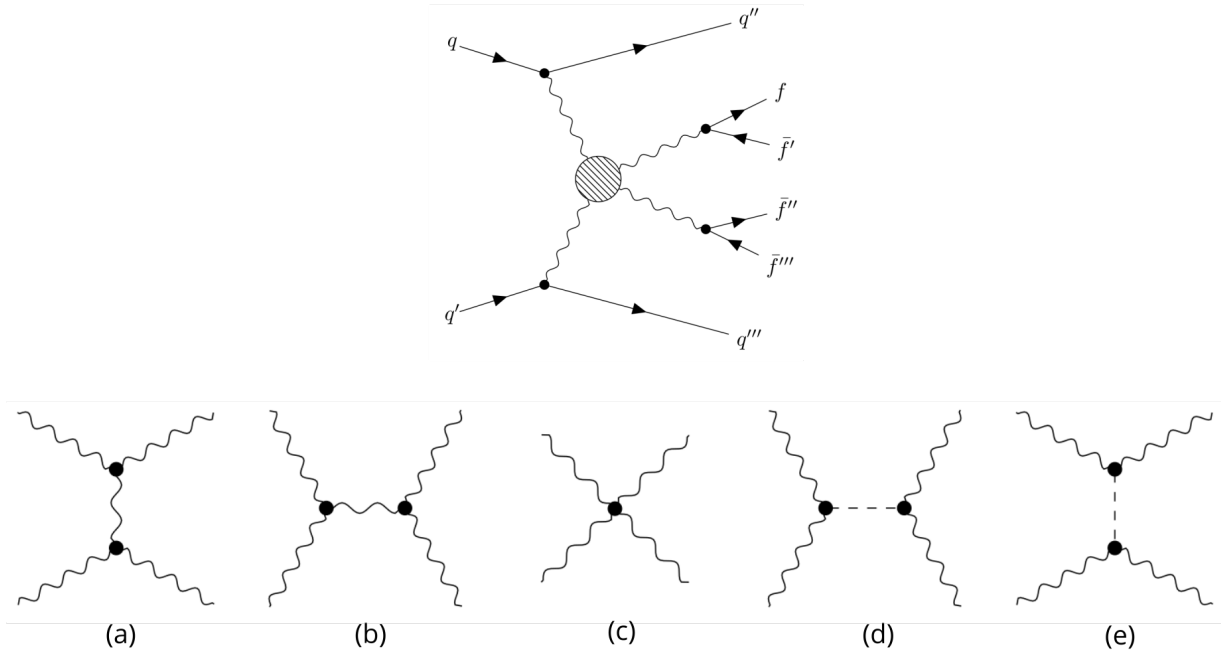
Figure 2.3: Structure of Full VBS process $qq \rightarrow VVjj \rightarrow 4ljj$ with two of the four leptons having a charge. The circle stands for the processes a to e which come from the non-Albanian gauge group $SU(2)$ for weak interactions in leading order $VV \rightarrow VV$ processes.[**Bittrich.27.05.2020**]

2.3 GM H5 Model

2.4 Vector Boson Scattering

Vector Boson Scattering(VBS) refers to the scattering of any electroweak gauge Boson V=$W^{\pm}$, Z, γ. This Definition includes diboson processes which makes it necessary to specify the finale state for VBS and diboson processes. The VBS finale state $VVjj$ is characterized by the two Bosons and two jets while diboson processes finale state only contains two Bosons VV in the finale state. Since gauge bosons have a short half-life of $3 \cdot 10^{-25}$s one needs to include the decay of the outgoing boson leading to the full process $qq \rightarrow VVjj \rightarrow 4ljj$ shown in figure 2.3. In leading order only quark-initiated diagrams produce vector bosons. These quarks are shifted by a small angle away from the beam axis resulting in the for the VBS process characteristic tagging jets. The couplings a to e in 2.3 are all electroweak interactions and based on there coupling structure produce a squared matrix element $|M^2| \propto \alpha_{EW}^6$. The α_{EW} stands for the combined coupling strength of the electroweak and electromagnetic interactions. These couplings can also be achieved by coupling structure $|M^2| \propto \alpha_{EW}^4 \alpha_S^2$,but these couplings however do not contribute to VBS processes. In the signal for VBS processes the diagrams with less than six electroweak diagrams are considered as Background defining the $VVjj - EW6$ processes. Some examples for the these processes can be seen in 2.4. How these processes

are selected will be discussed in the following chapter. The $W^\pm Z$ processes is dominated by EW and QCD interactions specifically the EFT Terms are only accounted for in the EW interactions.
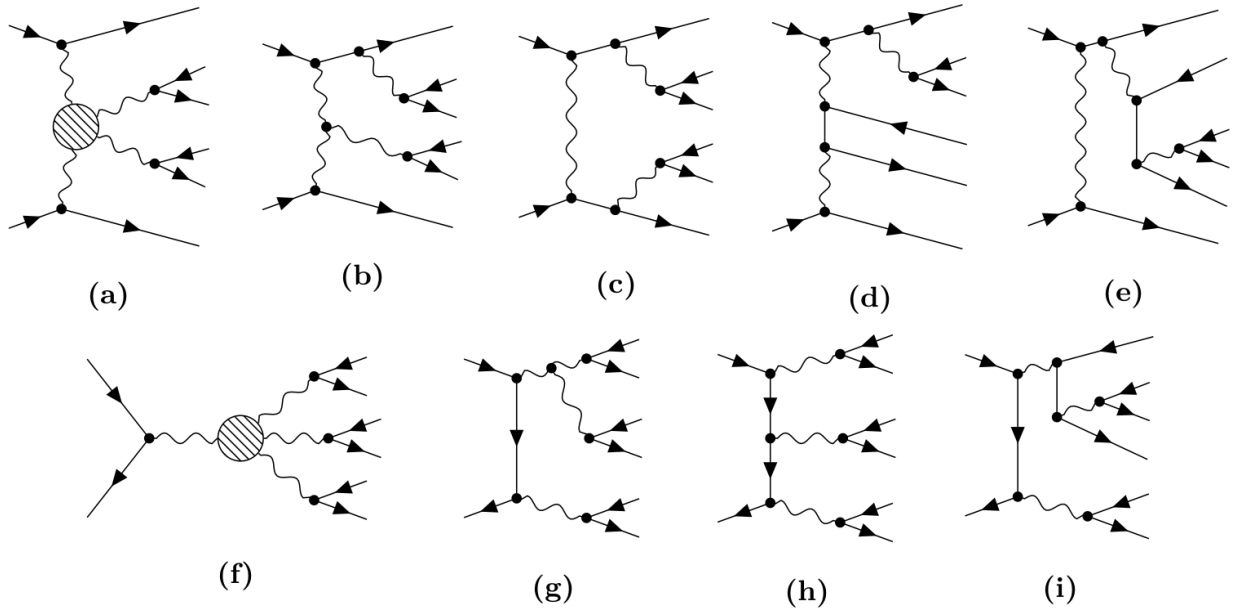
Figure 2.4: Example Feynman diagrams for VVjj-EW6 processes. The dashed circle stands for the Feynman diagrams a-e in Figure 2.3

3 Reproduction of Standard Model

3.1 Event Selection

Event selection criterion	lllvjj region	WZjj region	VBSSR
Event cleaning	√	√	√
GoodRunList	√	√	√
Trigger	√	√	√
Primary Vertex	√	√	√
lllvjj finale state			
≥ 2 jets	√	√	√
≥ 3 Z-Analysis leptons	√	√	√
One SFOC pair	√	√	√
l_W is in W-Analysis selection	√	√	√
Transverse momentum of leading leptons			
$p_T(l) > 25(27)GeV$	√	√	√
Transverse momentum of subleading jet			
$p_T(j_2) > 40GeV$	√	√	√
$M_T(W) > 30GeV$		√	√
$|M(ll) - 91.1876GeV| < 10GeV$		√	√
four Baseline leptons veto		√	√
b-jet veto		√	√
$M(jj) > 500GeV$			√
$\Delta Y(jj) > 2$			√

Table 3.1: Text [**Bittrich.27.05.2020**]

Event Selection is done in order to degrease background and get a clean signal process. VBS processes have a small cross-section around 1 fb resulting in a small event count. In the 2015 and 2016 Atlas run with 36 fb^{-1} not even 100 events produce VBS processes. There for one has to carefully select Events in order to get a meaningful signal process. The Events Selection is implemented as described in [**Bittrich.27.05.2020**] using the Common Analysis Framework(CAF). The Object selection however was already done in ELCore and account for the Event cleaning, GoodRunList, Trigger, Primary Vertex in Table 3.1 these cant be change in the CAF. Therefore, only the Event selection done in the CAF will be discussed. ELCore produces beam reconstruction level samples the Event Selection in the CAF is split into the three phase space regions lllvjj, WZjj and the VBS signal region(VBSSR). Even though the

regions are different the selection criteria overlap. The WZjj region use the selection criteria of the lllvjj as base and introduces new selection criteria. The same is true for the VBSSR which builds upon the WZjj region as show in Table 3.1.

lllvjj region: Only events with 3 or more leptons that pass the Z-analysis are chosen. The Leptons are then assigned to the decaying gauge boson. For this same flavour and opposite charge(SFOC) leptons pairs are chosen. The pair with invariant mass close to the Z Boson mass is assigned to the Z-Boson. The highest transverse momentum p_T lepton from the remaining leptons is assigned to the $W^{\pm}$-Boson and required to pass de W-analysis. Chosen leptons need a transverse momentum $p_T > 25(27)$ GeV for the 2015(2016) campaign for the events to pass the trigger threshold. Events have to have two or more events in order to be selected. These jets need to have $p_T(j) > 40$ GeV to be considered as tagging jets.

WZjj region: Additinal cuts are applied for the WZjj region in order to maximise $W^{\pm}Z$ contribution in the lllvjj final state. Some Events line ZZ diboson production are expected to produce an additional lepton therefore a four lepton Baseline veto is applied. Events where the jet is considered a b-jet are discarded to minimize $t\bar{t}$ and other t-quark contributions. The Transverse mass of the $W\pm$-Boson is required to be greater than $M_T(W) > 30$ GeV. The Z lepton pair has to have an invariant mass within 10 GeV of the Z-Boson mass $m_Z = 91.1876$.

VBSSR region: The resonance fitting is done in the VBSSR region. For this additional requirements must be added increasing WZjj-EW6 contribution compared to WZjj-EW4 and WZjj-EW5. For this two cuts for the tagging jets have to added. The invariant mass must be $M(jj) > 500$ GeV and the absolute rapidity difference hast be constraint $\Delta Y(jj) > 2$.

Figure 3.1 shows the cuts for the VBSSR region applied for the combined data from mc16d and mc16e with a combined luminosity of 102.7 fb^{-1}. These histograms will be combined to WZ + Background in the following Plots. Ideally one would use all campaigns mc16a, mc16d and mc16e with combined luminosity of 139 fb^{-1} to achieve the best statistic. For this Analysis the EFT Samples as well as the GM resonance samples have to be included resulting in to many Branches in the TQSampleTree than the current ROOT version 6.14.04 used by the CAF can process.

(a) **(b)**
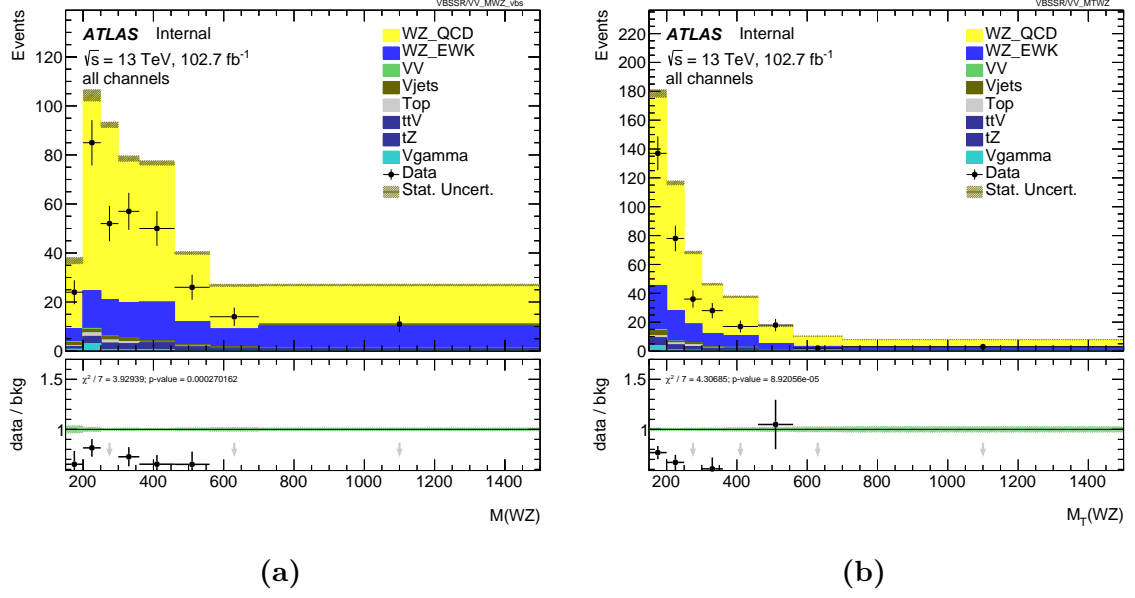
Figure 3.1: VBSSR region for a) invariant Mass, b) transverse mass. Showing reproduction of SM as well as the in section 2.4 discussed dominance of QCD and EW processes.

VBSSR	mc16d+mc16e	mc16a	SM
WZ QCD	356.8912 ± 2.4118	121.5475 ± 1.1721	144 ± 41
WZ EWK	91.2393 ± 0.4231	32.4363 ± 0.2522	24.9 ± 1.4
Background	27.2161 ± 2.0335	11.9691 ± 0.4701	31.1 ± 3.9
WZ SM + Background	475.3466 ± 3.2912	165.9529 ± 1.4050	200 ± 41

Table 3.2: Overwiev of Events in VBSSR region. mc16a is compared to the [**STDM**] for the reproduction of the SM EFT Limits. While the Resonance Fitting is done with the mc16e+mc16d data. The differences between the mc16a and the SM is like cause by some ELCore settings since the cuts possible in the CAF tool where replicated.

3.2 Standard Model EFT Limits

Erklärung

Hiermit erkläre ich, dass ich diese Arbeit im Rahmen der Betreuung am Institut für ??? Physik
ohne unzulässige Hilfe Dritter verfasst und alle Quellen als solche gekennzeichnet habe.

Vorname Nachname
Dresden, Monat 2019